International Conference on Applied Energy 2019
Aug 12-15, 2019, Västerås, Sweden
Paper ID: 997

THERMODYNAMIC ANALYSES OF DUAL-PRESSURE ORGANIC RANKINE CYCLES FOR OCEAN THERMAL ENERGY CONVERSION (OTEC)

Qiang Liu [1,*], Zhigang Lan [2], Ting Yu [2], Dashu Li [2], Yonghu Wu [2], Juan Yue [2]

1 State Key Laboratory of Petroleum Resources and Prospecting, Beijing Key Laboratory of Process Fluid Filtration and Separation, China University of Petroleum, Beijing, 102249, PR China (*Corresponding Author, qliu@cup.edu.cn)
2 CNOOC Research Institute Co. Ltd., Beijing 100028, PR China

ABSTRACT

Ocean thermal energy has been identified as a good thermal source for electric power generation especially for offshore oil and gas platforms and island energy security. Organic Rankine Cycles (ORCs) are promising systems for conversion ocean thermal energy to electricity; however, the thermal efficiencies still need to be increased. In this work, a dual-pressure ORC is used to improve the thermal efficiency of a closed ocean thermal energy conversion (OTEC) power plant. The evaporation and condensation temperatures of the dual-pressure ORCs are optimized to maximize the net power out. Compared to single-pressure ORCs, the dual-pressure ORCs can reduce the warm seawater temperature drop about 2 °C and generate 28-29% more net power. The working fluid with a higher critical temperature has a lower flow rate for the optimal condition. R600 produces slight high power than the other selected working fluids.

Keywords: dual-pressure Organic Rankine Cycle, ocean geothermal energy conversion (OTEC), thermodynamic analysis, parameter optimization, working fluid

NONMENCLATURE

Abbreviations	
CWP	Cold sea water pump
G	Generator
HPE	High pressure evaporator
HPP	High pressure pump
HPPH	High pressure preheater
HPT	High pressure turbine
LPE	Low pressure evaporator
LPPH	Low pressure preheater
LPT	Low pressure turbine
ORC	Organic Rankine cycle
OTEC	Ocean thermal energy conversion
WCC	Wet cooling condenser
WFP	Working fluid pump
WWP	Warm sea water pump
Symbols	
d	Diameter (m)
L	Pipe length (m)
m	Mass flow rate (kg s^{-1})
P	Power (kW)
Q	Heat flow (kW)
h	Specific enthalpy (kJ kg^{-1})
H	Head loss (m)
s	Specific entropy (KJ kg K^{-1})
W	Power (kW)
C_P	Isobaric heat capacity (kJ $kg^{-1}K^{-1}$)
η	efficiency

1. INTRODUCTION

Ocean temperature varies from 24 to 28 °C on surface and to 4–6°C at 1 km depths. The Ocean thermal energy refers to the thermal energy between surface warm seawater and deep cold seawater and has the distinctive features of being stable and being controllable. The ocean thermal power potential is estimated to be 87600 TWh/y [1]. The ocean thermal energy conversion (OTEC) has been identified as a good electrical power production strategy for island energy supply, offshore oil and gas platforms [2]. Organic Rankine Cycle (ORC) is a state-of-the-art technology that can generate power using ocean thermal energy at temperatures of 24-28°C. There have been a number of studies addressing OTEC performance

[1-3], characteristics [4-7], design criteria and types [8-13] for power generation systems.

The thermal efficiencies of OTEC power plants are still lower. How to improve the OTEC performance remains a crucial issue. The thermodynamic perfectness of a single pressure evaporation OTEC is relatively low. A dual-pressure ORC (DPORC) with a high-pressure and a low-pressure evaporation has a better match between the temperatures of the working fluid and the warm seawater which leads to an increase in the average heat absorption temperature and a decrease in the exergy losses during the evaporation [14]. The temperature drop of the warm seawater is lower for a single-pressure ORC; while the warm seawater can be cooled to a much lower temperature. This work focuses on the thermodynamic performance of dual-pressure ORCs for OTEC. The evaporation and condensation temperatures are simultaneously optimized to maximize the net power output. R218, R1234yf, R1234ze, R600a and R600 are selected as the working fluids. The thermodynamic performance is analyzed and the results are compared to find attractive working fluids.

2. MODEL

A schematic of a dual-pressure ORC using ocean thermal energy is shown in Fig. 1. The saturated working fluid from the water cooling condenser (WCC) outlet is pressurized by the working fluid feed pump (WFP) and then absorbs the sea water heat in the low-pressure preheater (LPPH). The working fluid is separated at the LPPH outlet. Part of the working fluid flows into the low-pressure evaporator (LPE). The other part of the working fluid is pressurized again to a higher pressure by the high-pressure feed pump (HPP) and then successively flows into the high-pressure preheater (HPPH) and the high-pressure evaporator (HPE). The high-pressure saturated vapor then expands in the high-pressure turbine (HPT). The superheated vapor exhausted from the HPT combines with the saturated vapor from the LPE, and then expands in the low-pressure turbine (LPT) to the condensation pressure. The exhaust vapor from the LPT is then condensed by the cold sea water to the saturated liquid in the WCC. Compared to a single-pressure ORC, the warm sea water can be cooled to a lower temperature in a dual-pressure ORC. The operating parameters and boundary conditions of the OTEC power plant are listed in Table 1.

Mass and energy balances for any control volume at steady state with negligible potential and kinetic energy changes can be expressed as

$$\Sigma\dot{m}_{\text{in}} = \Sigma\dot{m}_{\text{out}} \tag{1}$$

$$\dot{Q} - \dot{W} = \Sigma\dot{m}_{\text{in}}h_{\text{in}} - \Sigma\dot{m}_{\text{out}}h_{\text{out}} \tag{2}$$

The net power output of the dual-pressure ORC is calculated as

$$\dot{W}_{\text{net}} = \dot{W}_{\text{T}} - \dot{W}_{\text{WFP}} - \dot{W}_{\text{WWP}} - \dot{W}_{\text{CWP}} \tag{3}$$

where $\dot{W}_{\text{T}}$ is the power generated by the high-pressure and low-pressure turbines, $\dot{W}_{\text{WWP}}$ is the power consumed by the warm sea water pump, $\dot{W}_{\text{CWP}}$ is the power consumed by the cold sea water pump, and $\dot{W}_{\text{WFP}}$ is the power consumed by the working fluid pumps.

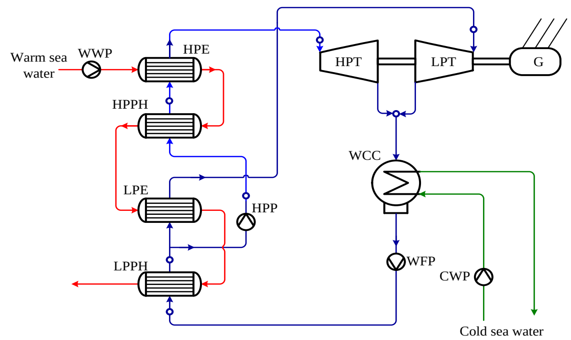

Fig. 1 Schematic of a dual-pressure OTEC system

The power consumed by the warm sea water pump is

$$\dot{W}_{\text{WWP}} = \frac{\dot{m}_{\text{WW}} g H_{\text{WWP}}}{\eta_{\text{SWP}}} \tag{4}$$

where $\dot{m}_{\text{WW}}$ is the warm sea water flow rate, H_{WWP} is the warm seawater pump head and η_{SWP} is the sea water pump efficiency.

The warm seawater head loss is defined as

$$H_{\text{WWP}} = 6.82\frac{L_{\text{WW}}}{d_{\text{WW}}^{1.17}}\left(\frac{v_{\text{WW}}}{100}\right)^{1.85} + H_{\text{WW,E}} \tag{5}$$

where L_{WW} is the warm sea water pipe length, d_{WW} is the warm seawater pipe diameter, v_{WW} is the warm sea water velocity, and $H_{\text{WW,E}}$ is the head loss in the evaporator.

The power consumed by the cold sea water pump is

$$\dot{W}_{\text{CWP}} = \frac{\dot{m}_{\text{CW}} g H_{\text{CWP}}}{\eta_{\text{SWP}}} \tag{6}$$

The cold sea water flow rate can be calculated as

$$\dot{m}_{\text{CW}} = \frac{\dot{Q}_{\text{COND}}}{\Delta T_{\text{CW}} c_{\text{CW},p}} \tag{7}$$

The cold seawater pump head is defined as

$$H_{\text{CWP}} = H_{\text{CW,SP}} + H_{\text{CW,D}} + H_{\text{CW,C}} \tag{8}$$

The friction loss of the straight pipe is

$$H_{\text{CW,SP}} = 6.82\frac{L_{\text{CW}}}{d_{\text{CW}}^{1.17}}\left(\frac{v_{\text{CW}}}{100}\right)^{1.85} \tag{9}$$

The pressure difference caused by the density difference between the warm and the cold sea water is

$$H_{\mathrm{CW,D}} = L_{\mathrm{CW}} - \frac{1}{2\rho_{\mathrm{CW}}}\left(\rho_{\mathrm{CW}} + \rho_{\mathrm{WW}}\right)L_{\mathrm{CW}} \qquad (10)$$

where L_{CW} is the COLD sea water pipe length, d_{CW} is the cold seawater pipe diameter, v_{CW} is the cold sea water velocity, ρ_{CW} is the cold seawater density, ρ_{WW} is the warm seawater density and $H_{\mathrm{CW,C}}$ is the head loss in the condenser.

Table 1 Boundary conditions of the OTEC power plant.

Parameters	Value
Warm sea water inlet temperature	28 °C
Cold sea water temperature	4 °C
Warm sea water pipe length	200 m
Cold sea water pipe length	1000 m
Pinch point difference in the evaporator	1.5 °C
Pinch point difference in the IHE and condenser	1.5 °C
Turbine mechanical efficiency	98%
Generator efficiency	98%
Isentropic efficiency of working fluid pumps	80%
Sea water pump efficiency	80%
Isentropic efficiency of turbine	85%
Warm seawater head loss in evaporator	1 m
Cold seawater head loss in condenser	1.5 m
Warm sea water flow rate	1000 kg/s

The thermal efficiency of the OTEC power plant is defined as

$$\eta_{\mathrm{th}} = \frac{\dot{W}_{\mathrm{net}}}{\dot{m}_{\mathrm{WW}} c_{\mathrm{WW},p} \Delta T_{\mathrm{WW}}} \qquad (11)$$

3. RESULTS AND DISCUSSION

The evaporation and condensation temperatures are optimized simultaneously to maximize the net power output using the generalized reduced gradient (GRG) method [15-16]. Fig. 2 shows the temperature drop of the warm seawater in single-pressure ORCs and dual-pressure ORCs with the selected 5 working fluids for the optimal conditions. Compared to a single-pressure ORC, the temperature drop of the warm seawater is increased by about 2.2°C due to a low pressure evaporation loop in a dual-pressure ORC. Thus, the working fluid flow rates are significantly increased for DPORCs as shown in Fig. 3. The DPORCs use about 26-28% more working fluid for the optimal conditions than single pressure ORCs. The evaporation latent heats are higher for the working fluids with higher critical temperatures; therefore, the working fluid flow rates decrease. Among the selected 5 working fluids, the critical temperature of R600 (butane) is the highest while the flow rate is the lowest.

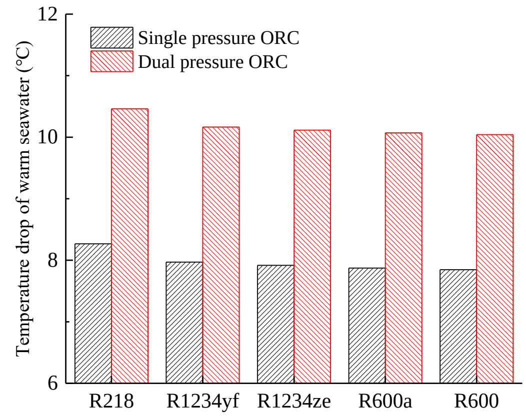

Fig. 2 Temperature drop of warm seawater

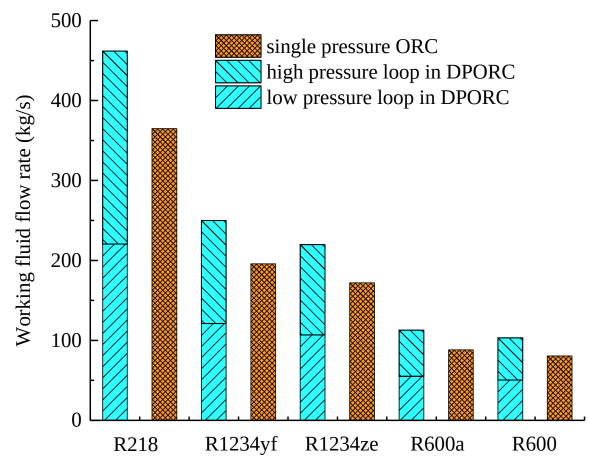

Fig. 3 Flow rates for various working fluid

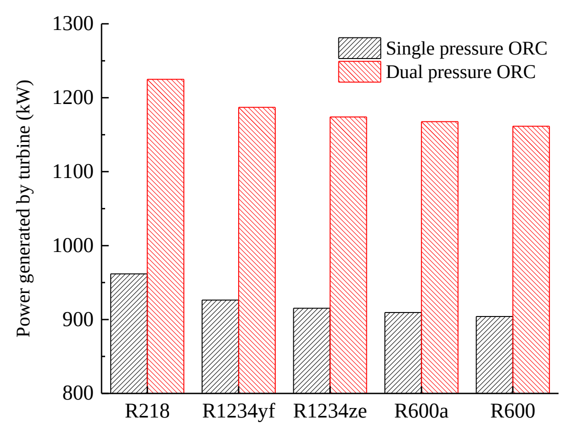

Fig. 4 Turbine power outputs for various working fluid

Fig. 4 shows the power generated by the turbine and the maximized net power for the single-pressure and dual-pressure ORCs with the selected working fluids. The turbine using the working fluids with higher critical temperature generates higher work. The turbine using R218 generates the maximum power; however, the working fluid pumps and the cold seawater pump also consume the maximum power due to the highest working fluid flow rate. A dual-pressure ORC can generate 27% more power than an ORC.

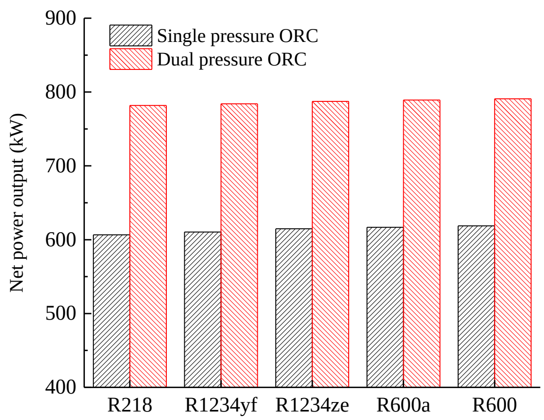

Fig. 5 Net power outputs for various working fluid

Fig. 5 shows the net power output for dual-pressure and single-pressure ORCs with the selected working fluid. 32-37% of the power generated by the turbine are consumed by the pumps. The net power outputs generated by the selected working fluids are very close. Dual-pressure ORCs generate 28-29% more net power than single-pressure ORCs.

4. CONCLUSIONS

The evaporation and condensation temperatures are optimized simultaneously to maximize the net power output for OTEC power plants. The working fluid with a lower critical temperature has a higher flow rate and then generates a higher turbine power; however, the pumps also consume more power. The parasitic power consumed by the pumps accounts for 32-37% of the turbine power output. A dual-pressure ORC can increase the warm seawater temperature drop about 2 °C, compared to a single-pressure ORC. The dual-pressure ORCs generate 28-29% more net power than single-pressure ORCs. The maximum power is produced by R600.

ACKNOWLEDGEMENT

This work was supported by the National Natural Science Foundation of China (Grant Nos. 51506223 and 51736005), and the CNOOC (China) CO. LTD (No. YXKY-2018-ZY-09).

REFERENCE

[1] Khan N, Kalair A, Abas N, Haider A. Review of ocean tidal, wave and thermal energy technologies. Renew Sustain Energy Rev 2017; 72: 590-604.

[2] Li DS, Yue J, Zhang L, Duan XL. Numerical study on ocean thermal energy conversion system. J Renew Sustain Energy 2018; 10: 044501.

[3] Nithesh KG, Chatterjee D. Numerical prediction of the performance of radial inflow turbine designed for ocean thermal energy conversion system. Appl Energy 2016; 167: 1-16.

[4] Wang M, Jing R, Zhang HR, Meng C, Li N, Zhao YR. An innovative Organic Rankine Cycle (ORC) based Ocean Thermal Energy Conversion (OTEC) system with performance simulation and multi-objective optimization. Appl Therm Eng 2018; 145: 743-54.

[5] Devault DA, Péné-Annette A. Analysis of the environmental issues concerning the deployment of an OTEC power plant in Martinique. Environ Sci Pollut Res 2017

[6] Sun FM, Ikegami Y, Jia BJ, Arima H. Optimization design and exergy analysis of organic rankine cycle in ocean thermal energy conversion. Appl Ocean Res 2012; 35:38-46.

[7] Yang MH, Yeh RH. Analysis of optimization in an OTEC plant using organic Rankine cycle. Renew Energy 2014; 68: 25-34.

[8] Uehara H, Ikegami Y. Optimization of a closed-cycle OTEC system. J Sol Energy Eng 1990; 112: 247-56.

[9] Bernardoni C, Binotti M, Giostri A. Techno-economic analysis of closed OTEC cycles for power generation. Int Renew Energy 2019; 132: 1018-33.

[10] Yamada N, Hoshi A, Ikegami Y. Performance simulation of solar-boosted ocean thermal energy conversion plant. Renew Energy 2009; 34:1752-8.

[11] Zhang W, Li Y, Wu XN, Guo SH. Review of the applied mechanical problems in ocean thermal energy conversion. Renew Sustain Energy Rev 2018; 93: 231-44.

[12] Yamada N,Hoshi A, Ikegami Y. Performance simulation of solar-boosted ocean thermal energy conversion plant. Renew Energy 2009; 34: 1752-8.

[13] Ikegami Y, Yasunaga T, Morisaki T. Ocean Thermal Energy Conversion Using Double-Stage Rankine Cycle. J Mar Sci Eng 2018; 6: 21. doi:10.3390/jmse6010021

[14] Sun J, Liu Q, Duan YY. Effects of reinjection temperature on thermodynaminc performance of dual-pressure and sigle-pressure geothermal ORCs. Energy Procedia 2019; 158: 6016-23.

[15] Liu Q, Duan YY, Yang Z. Effect of condensation temperature glide on the performance of organic

Rankine cycles with zeotropic mixture working fluids. Appl Energy 2014;115:394-404.
[16] Liu Q, Shen AJ, Duan YY. Parametric optimization and performance analyses of geothermal organic Rankine cycles using R600a/R601a mixtures as working fluids. Appl Energy 2015; 148: 410-20.

